JTTEE5 18:1014–1021
DOI: 10.1007/s11666-009-9368-4

Peer Reviewed

Modeling of Thermal Spraying Heat Transfer Processes by Exodus Stochastic Method

Milan Honner and Jan Sroub

(Submitted January 29, 2009; in revised form July 8, 2009)

This article deals with the application of the stochastic Exodus method for modelling of thermal spraying heat transfer processes and for solving direct and indirect problems. The Exodus stochastic method has an advantage in straightforward solving of the transient inverse heat transfer multi-dimensional problems over other methods based on iterative fittings procedures used for example by finite element methods (FEM). Theoretical background of the method is introduced. Application capabilities of the method are shown on the example of high velocity oxygen fuel thermal spraying heat transfer process analysis. Comparisons with results of FEM computational method application are presented.

Keywords diagnostics and control, HVOF process, influence of process parameters

1. Introduction

Properties of coatings produced by thermal spraying technologies are influenced by a number of parameters (Ref 1, 2). From the thermal point of view, the spraying deposition process can be divided into three processes. First, heat transfer into the substrate consists of the effect of the hot fluid as impact heating flow. Further, the thermal energy of the molten powder deposited on the surface is transmitted mainly by conduction to the substrate or is lost by radiation to the surrounding environment. The kinetic energy of the accelerated powder particles is also transformed into heat during the impact, when the motion of the particle is stopped and highly laterally deposited on the clean substrate or on the already solidified earlier particles. The above-mentioned processes manifest themselves as the surface dynamic temperature field of the sample being coated. Therefore, attention is given to methods enabling heat transfer processes and temperature on the sample surface to be analyzed. Application of temperature measurement techniques in conjunction with computer simulation can reveal and distinguish the effect of the above-mentioned heat transfer processes (Ref 3).

The common feature of thermal spraying technologies is the fact that the material's surface temperature is difficult to measure directly, using either contact or non-contact methods. Difficulties in the application of contact methods such as thermocouples can be found, for example, in the undesirable influence on the surface temperature by the sensor placement. Another difficulty is caused

Milan Honner and **Jan Sroub**, Department of Physics, University of West Bohemia in Pilsen, Plzen 30614, Czech Republic. Contact e-mail: honner@ntc.zcu.cz.

Nomenclature

Latin Alphabet

a	thermal diffusivity (m^2 s^{-1})
b	transition probability (–)
$\boldsymbol{B}$	transition probabilities matrix (–)
Bi	Biot number (–)
c	Heat capacity (J kg^{-1} K^{-1})
f	Surface temperature (K)
Fo	Fourier number (–)
h	distance to neighboring node (m)
L	characteristic length (–)
n	number of nodes (–)
n	dimensionless distances to neighboring node (–)
p	random walk probability (–)
P	random walk probability matrix (–)
t	temperature (K)

Greek Alphabet

δFo	step of Fourier number (–)
$\Delta\tau$	time step (s)
λ	thermal conductivity (W m^{-1} K^{-1})
ρ	density (kg m^{-3})
τ	time (s)

Indexes

abs	absorption
refl	reflection
A	relating to absorbing nodes
N	relating to non-absorbing nodes

Abbreviations

FEM	finite element method
HVOF	high velocity oxygen fuel

by the usually much better thermal contact of the sensor with the surrounding fluid than with the material surface to be measured. Problems in non-contact methods, based on sensing surface thermal radiation, are caused for example by the plasma between the sensor and the heat-treated surface or by emissivity of the surface, which changes during the deposition.

In such cases, an inverse surface temperature measurement is a suitable alternative. This is based on the contact measurement of temperature at exact locations under the sample surface. The surface temperature evolution over time and distribution in space is subsequently determined by the application of a numerical simulation method as an inverse problem.

Effective methods for resolving inverse problems have allowed researchers to simplify experiments considerably, and to increase the accuracy and confidence of results in experimental data processing (Ref 4, 5). Rapid development of computational systems based on finite element methods and their increasing capabilities has found numerous applications in resolving the inverse problems (Ref 6) and in the simulation of surface modification technologies (Ref 7). However, the algorithms often used are based on iterative fitting of the computed temperatures at selected material locations to the measured ones. Such a procedure is time consuming and usually also ambiguous, especially concerning the transient problems. Therefore, there is still the demand for a method that could enable straightforward solving of the transient inverse heat transfer multi-dimensional problems (Ref 8) by some direct and exactly defined routine. The stochastic Exodus method modification for the transient problems presented in this paper aspires to fill the gap and to propose its capabilities for special problems.

A modification of the Monte Carlo method (Ref 9), the Exodus method was introduced by Emery and Carson (Ref 10). The Exodus method can be used to simulate deterministic or stochastic processes in discrete stochastic models. The stochastic model system consists of components or subsystems which send walkers between each other. Walkers are randomly moving particles which transport energy, mass or data pulses from the surface inwards and reversely.

The Exodus method is not dependent on a random number generator. The method has been found to yield more accurate results with less computing time as compared to the original Monte Carlo method. With regards to the Monte Carlo method its accuracy is dependent on the number of sequentially launched walkers that are all absorbed in absorbing nodes. On contrary, the accuracy of the Exodus method (all walkers are launched together) is dependent also on the number of walkers absorbed in absorbing nodes at the time of the solving termination. Usually 98% absorption of all launched walkers is used as a level to stop the solution progress.

The Exodus method is a numerical technique which is capable of providing an exact solution. It is based on the description of thermal fields by Markov's chains (Ref 11). The Exodus method provides results with the same degree of accuracy as those obtained using the finite difference method. However, the Exodus method enables to solve an inverse problem in one straightforward procedure that appears the main advantage of this method.

A simple introduction to the Exodus method for steady state was presented in Ref 12 and 13. In this paper, the transient method for analyses of thermal spraying heat transfer processes is described in detail for the direct problem and especially for the inverse problem, where the method gains advantages over the deterministic methods. The application capabilities of the method will be shown in the example of the HVOF thermal spraying heat transfer process analysis. Finally, a comparison with the results of the FEM computational method (Ref 3) will be presented.

Peer Reviewed

2. Theory

In this section, the theoretical background for the Exodus method is briefly presented. The method is applied to the heat transfer equation in the rectangular solution region.

A system consisting of n nodes is described by the square random walk probabilities n-th dimension matrix $\boldsymbol{P}$. The element p_{ij} of the matrix $\boldsymbol{P}$ is a random walk probability of the walker from node i to j. Row sums of the matrix $\boldsymbol{P}$ are 1. The matrix $\boldsymbol{P}$ is a band matrix for systems in which walkers can walk only to the neighboring nodes.

2.1 Random Walk Probabilities

Applying the Exodus method in finding the solution usually involves the following three steps (Ref 12):

1. Obtaining the random walk probabilities from the finite difference equivalent of the partial differential equation describing the problem.
2. Using the Exodus method along with the random walk probabilities in calculating the transition probabilities.
3. Determining the temperature at the point of interest using the transition probabilities and the boundary conditions.

Suppose the Exodus method is to be applied in solving the heat transfer equation

$$a\left(\frac{\partial^2 t}{\partial x^2}+\frac{\partial^2 t}{\partial y^2}\right)=\frac{\partial t}{\partial \tau}, \qquad \text{(Eq 1)}$$

where a is thermal diffusivity, t temperature and τ time. Equation 1 is discretized by the mesh of the rectangular solution region, where h_{x+}, h_{x-}, h_{y+}, h_{y-} are the distances to neighboring nodes (Fig. 1)

$$\begin{aligned}
\frac{\partial^2 t}{\partial x^2}&=\frac{2}{h_{x+}+h_{x-}}\left(\frac{t_{i+1,j,k}-t_{i,j,k}}{h_{x+}}-\frac{t_{i,j,k}-t_{i-1,j,k}}{h_{x-}}\right),\\
\frac{\partial^2 t}{\partial y^2}&=\frac{2}{h_{y+}+h_{y-}}\left(\frac{t_{i,j+1,k}-t_{i,j,k}}{h_{y+}}-\frac{t_{i,j,k}-t_{i,j-1,k}}{h_{y-}}\right),\\
\frac{\partial t}{\partial \tau}&=\frac{1}{\Delta\tau}\left(t_{i,j,k+1}-t_{i,j,k}\right).
\end{aligned} \qquad \text{(Eq 2)}$$

The finite difference equivalent of (1) is therefore

$$\frac{2a\Delta\tau}{h_{x+}(h_{x+}+h_{x-})}t_{i+1,j,k}+\frac{2a\Delta\tau}{h_{x-}(h_{x+}+h_{x-})}t_{i-1,j,k}+\frac{2a\Delta\tau}{h_{y+}(h_{y+}+h_{y-})}t_{i,j+1,k}+\frac{2a\Delta\tau}{h_{y-}(h_{y+}+h_{y-})}t_{i,j-1,k}$$
$$+\left(1-\frac{2a\Delta\tau}{h_{x+}(h_{x+}+h_{x-})}-\frac{2a\Delta\tau}{h_{x-}(h_{x+}+h_{x-})}-\frac{2a\Delta\tau}{h_{y+}(h_{y+}+h_{y-})}-\frac{2a\Delta\tau}{h_{y-}(h_{y+}+h_{y-})}\right)t_{i,j,k}=t_{i,j,k+1} \quad \text{(Eq 3)}$$

Equation 3 is expanded by the square characteristic length L^2 and there are applied dimensionless segments n and the step of Fourier number $\Delta Fo = \lambda\Delta\tau(\rho c)^{-1}\ L^{-2}$, where λ (W m^{-2} K^{-1}) is thermal conductivity, c (J kg^{-1} K^{-1}) is heat capacity and ρ (kg m^{-3}) is density.

$$n_{x+}=\frac{h_{x+}}{L},\quad n_{x-}=\frac{h_{x-}}{L},\quad n_{y+}=\frac{h_{y+}}{L},\quad n_{y-}=\frac{h_{y-}}{L}, \quad \text{(Eq 4)}$$

$$\frac{2\Delta Fo}{n_{x+}(n_{x+}+n_{x-})}t_{i+1,j,k}+\frac{2\Delta Fo}{n_{x-}(n_{x+}+n_{x-})}t_{i-1,j,k}+\frac{2\Delta Fo}{n_{y+}(n_{y+}+n_{y-})}t_{i,j+1,k}+\frac{2\Delta Fo}{n_{y-}(n_{y+}+n_{y-})}t_{i,j-1,k}$$
$$+\left(1-\frac{2\Delta Fo}{n_{x+}(n_{x+}+n_{x-})}-\frac{2\Delta Fo}{n_{x-}(n_{x+}+n_{x-})}-\frac{2\Delta Fo}{n_{y+}(n_{y+}+n_{y-})}-\frac{2\Delta Fo}{n_{y-}(n_{y+}+n_{y-})}\right)t_{i,j,k}=t_{i,j,k+1} \quad \text{(Eq 5)}$$

From this difference equivalent (5) we obtain the random walk probabilities

$$p_{x+}=\frac{2\Delta Fo}{\Delta n_{x+}(\Delta n_{x+}+\Delta n_{x-})},\quad p_{x-}=\frac{2\Delta Fo}{\Delta n_{x-}(\Delta n_{x+}+\Delta n_{x-})},$$
$$p_{y+}=\frac{2\Delta Fo}{\Delta n_{y+}(\Delta n_{y+}+\Delta n_{y-})},\quad p_{y+}=\frac{2\Delta Fo}{\Delta n_{y-}(\Delta n_{y+}+\Delta n_{y-})} \quad \text{(Eq 6)}$$

and the probability of the stay in the node is

$$p_t=1-(p_{x+}+p_{x-}+p_{y+}+p_{y-}). \quad \text{(Eq 7)}$$

2.2 Probability of Absorption and Reflection

Boundary conditions are represented by the absorption and reflection probability at the considered region's boundaries. The surrounding environment's temperature makes up a part of the discretization grid throughout the set of absorbing nodes. Generally, the boundary heat transfer equation is

$$-\frac{\partial t}{\partial n}=\frac{Bi}{L}(t_i-f_i), \quad \text{(Eq 8)}$$

in which Bi is the Biot number, t_i is the surface temperature and f_i is the temperature of the fluid exchanging heat with the surface by convection. Equation 8 can be written in its difference form

$$-\frac{t_i-t_{i+1}}{h}=\frac{Bi}{L}(t_i-f_i), \quad \text{(Eq 9)}$$

where $Bi = \alpha L\lambda^{-1}$, where α (W m^{-2} K^{-1}) is the heat transfer coefficient and f is the temperature at the boundary. If length h is expressed as one mth of the characteristic length L, then after ordering

$$t_i=\frac{m}{Bi+m}t_{i+1}+\frac{Bi}{Bi+m}f_i=p_{\text{refl}}t_{i+1}+p_{\text{abs}}f_i. \quad \text{(Eq 10)}$$

Thus, the probability of absorption and reflection representing convection heat transfer are

$$p_{\text{refl}}=\frac{m}{Bi+m},\quad p_{\text{abs}}=\frac{Bi}{Bi+m}. \quad \text{(Eq 11)}$$

2.3 Transition Probabilities

To apply the Exodus method, let b_i be the number of walkers in node i. The initial transition probabilities vector is defined as

$$\boldsymbol{b}^{(0)}=\left[b_1^{(0)},b_2^{(0)},\ldots,b_n^{(0)}\right], \quad \text{(Eq 12)}$$

where

$$\begin{aligned} b_i&=1 \quad \text{for } i=j,\\ b_i&=0 \quad \text{for } i\neq j, \end{aligned} \quad \text{(Eq 13)}$$

As the initial transition probabilities vector is defined, the transition probabilities in the first time step is calculated

$$\boldsymbol{b}^{(1)}=\boldsymbol{b}^{(0)}\cdot\boldsymbol{P}, \quad \text{(Eq 14)}$$

similarly for the kth time step

$$\boldsymbol{b}^{(k)}=\boldsymbol{b}^{(k-1)}\cdot\boldsymbol{P}. \quad \text{(Eq 15)}$$

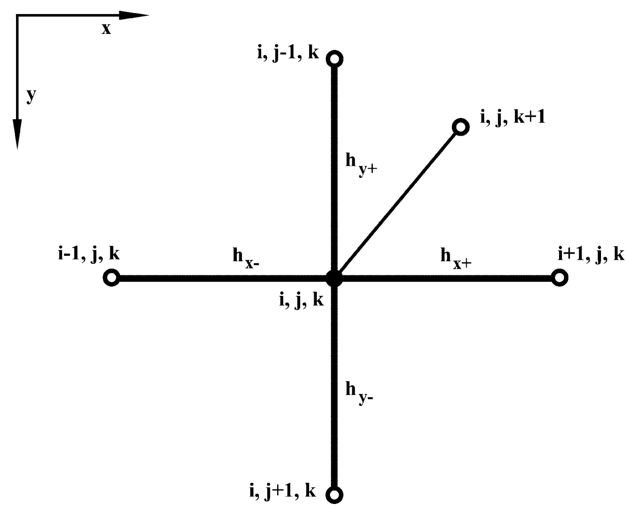

Fig. 1 Definition of parameters and indexes in relation to the computational grid—surrounding of general node

This gives

$$\boldsymbol{b}^{(k)} = \boldsymbol{b}^{(0)} \cdot \boldsymbol{P}^{k}. \qquad \text{(Eq 16)}$$

If computation of more nodal temperatures is required in one run, then the transition probabilities matrix $\boldsymbol{B}$ is used. It consists of row vectors $\boldsymbol{b}^{(0)}$

$$\boldsymbol{B}^{(0)} = \left[\boldsymbol{b}_1^{(0)^T}, \boldsymbol{b}_2^{(0)^T}, \ldots, \boldsymbol{b}_n^{(0)^T}\right]^T. \qquad \text{(Eq 17)}$$

The calculation procedure with $\boldsymbol{B}$ is the same as with $\boldsymbol{b}$, as

$$\boldsymbol{B}^{(k)} = \boldsymbol{B}^{(0)} \cdot \boldsymbol{P}^{k}. \qquad \text{(Eq 18)}$$

2.4 Direct Problems

Random walk probabilities from each node to all neighboring nodes for the selected mesh, set of thermo-physical parameters and time step will be specified from elementary thermal balances. At the same time, we set the transition probabilities.

The solution of the transient direct problem with the Dirichlet boundary condition and internal heat source is obtained as

$$\boldsymbol{t}^{(k)} = \boldsymbol{B}^{(k)} \cdot \boldsymbol{f}. \qquad \text{(Eq 19)}$$

If the matrix $\boldsymbol{B}$ is reordered in every time step, then the first columns will contain values corresponding with the absorbing nodes and the remaining columns will contain values corresponding with the non-absorbing nodes. Then the matrix $\boldsymbol{B}$ is divided into two parts

$$\boldsymbol{B}^{(k)} = \left[\boldsymbol{B}_{\mathrm{A}}^{(k)} \vdots \boldsymbol{B}_{\mathrm{N}}^{(k)}\right]. \qquad \text{(Eq 20)}$$

The vector $\boldsymbol{f}$ is reordered in the same manner as $\boldsymbol{B}$

$$\boldsymbol{f}^{T} = \left[\boldsymbol{f}_{\mathrm{A}} \vdots \boldsymbol{f}_{\mathrm{N}}\right] \qquad \text{(Eq 21)}$$

and matrix $\boldsymbol{N}$ and $\boldsymbol{q}$ as well. Then the solution is written

$$\boldsymbol{t}^{(k)} = \boldsymbol{B}_{\mathrm{A}}^{(k)} \cdot \boldsymbol{f}_{\mathrm{A}} + \boldsymbol{B}_{\mathrm{N}}^{(k)} \cdot \boldsymbol{f}_{\mathrm{N}}, \qquad \text{(Eq 22)}$$

where $\boldsymbol{f}_{\mathrm{A}}$ is the boundary conditions vector and $\boldsymbol{f}_{\mathrm{N}}$ is the initial conditions vector.

The problem with the transient boundary condition must be solved step by step. To obtain a temperature or other thermal characteristic, it is necessary to know the vector $\boldsymbol{b}^{(k)}$ in all previous time steps. The thermal characteristic in time step $k1$ is written as the sum of all previous time step increments

$$\boldsymbol{t}^{(k1)} = \sum_{k=1}^{k1} \left(\boldsymbol{B}^{(k)} - \boldsymbol{B}^{(k-1)}\right) \cdot \boldsymbol{f}^{(k1-k+1)}. \qquad \text{(Eq 23)}$$

If the matrix $\boldsymbol{B}$ is separated into parts corresponding with the absorbing and non-absorbing nodes, then the equation can be rewritten as

$$\boldsymbol{t}^{(k1)} = \sum_{k=1}^{k1} \left(\boldsymbol{B}_{\mathrm{A}}^{(k)} - \boldsymbol{B}_{\mathrm{A}}^{(k-1)}\right) \cdot \boldsymbol{f}_{\mathrm{A}}^{(k1-k+1)} + \boldsymbol{B}_{\mathrm{N}}^{(k1)} \cdot \boldsymbol{f}_{\mathrm{N}}. \qquad \text{(Eq 24)}$$

2.5 Inverse Problems

The inverse problem consists in finding the boundary conditions with respect to the defined evolution of temperature in the internal node. Zero internal sources are supposed for problem simplification. While in the case of direct problem we are able to compute the whole temperature field based on any number of boundary conditions, in the case of the inverse problem we are limited to a number of results equal to a number of different input temperature evolutions in internal nodes.

Consider the temperature time evolutions given in internal nodes of the region, ordered to vectors $\boldsymbol{t}^{(k)}$. If a steady boundary condition is supposed, the solution is Eq 22 with unknown vector $\boldsymbol{f}_{\mathrm{A}}$. Matrixes $\boldsymbol{B}_{\mathrm{A}}^{(k)}$ and $\boldsymbol{B}_{\mathrm{N}}^{(k)}$ are defined in the same way as for the direct problem. The aim is to find $\boldsymbol{f}_{\mathrm{A}}$ containing values of the boundary condition. From Eq 22, the vector of the boundary condition

$$\boldsymbol{f}_{\mathrm{A}}^{(k)} = \left(\boldsymbol{B}_{\mathrm{A}}^{(k)}\right)^{-1} \cdot \left(\boldsymbol{t}^{(k)} - \boldsymbol{B}_{\mathrm{N}}^{(k)} \cdot \boldsymbol{f}_{\mathrm{N}}\right), \qquad \text{(Eq 25)}$$

is computed for all time steps $k = 1, 2, \ldots, k1$.

The solution of the inverse problem with transient boundary condition starts from the solution of the corresponding direct problem. Using this notation, it is possible to write the following equation

$$\boldsymbol{t}_{\mathrm{A}}^{(k1)} = \sum_{k=1}^{k1} \left(\boldsymbol{B}_{\mathrm{A}}^{(k)} - \boldsymbol{B}_{\mathrm{A}}^{(k-1)}\right) \cdot \boldsymbol{f}_{\mathrm{A}}^{(k1-k+1)} + \sum_{k=1}^{k1} \left(\boldsymbol{B}_{\mathrm{N}}^{(k)} - \boldsymbol{B}_{\mathrm{N}}^{(k-1)}\right) \cdot \boldsymbol{f}_{\mathrm{N}}^{(k1-k+1)}. \qquad \text{(Eq 26)}$$

First, we compute the solution of $\boldsymbol{f}^{(1)}$ for known $\boldsymbol{t}^{(1)}$ from Eq 26 for $k1 = 1$

$$\boldsymbol{f}_{\mathrm{A}}^{(1)} = \left(\boldsymbol{B}_{\mathrm{A}}^{(1)} - \boldsymbol{B}_{\mathrm{A}}^{(0)}\right)^{-1} \cdot \left[\boldsymbol{t}_{\mathrm{A}}^{(1)} - \left(\boldsymbol{B}_{\mathrm{N}}^{(1)} - \boldsymbol{B}_{\mathrm{N}}^{(0)}\right) \cdot \boldsymbol{f}_{\mathrm{N}}^{(1)}\right]. \qquad \text{(Eq 27)}$$

Peer Reviewed

After rearrangement, we set $f_A^{(k1)}$, for $k1 > 1$

$$f_A^{(k1)} = \left(B_A^{(1)} - B_A^{(0)}\right)^{-1} \cdot \left[t_A^{(k1)} - \sum_{k=2}^{k1} \left(B_A^{(k)} - B_A^{(k-1)}\right) \times f_A^{(k1-k+1)} - \sum_{k=1}^{k1} \left(B_N^{(k)} - B_N^{(k-1)}\right) \cdot f_N^{(k1-k+1)} \right]. \tag{Eq 28}$$

Vectors t_A, f_N and matrix B in Eq 28 are set in the same way as in the direct problem. Values f_A on the right side are known from the previous time steps.

3. Application Example

The application of the Exodus method will be demonstrated in the example of heat transfer during HVOF deposition of protective coatings.

3.1 Measurement

In the inverse heat conduction problem, temperature sensors are embedded within the sample volume and the surface temperature and heat flux are evaluated. The thermal process was investigated on a steel sample (30 × 70 × 100 mm), where the largest side was coated. The linear trajectory of the gun was chosen along the lengthwise axis of the sample right above the measuring positions at a distance of 380 mm from the surface. Temperature was measured by 0.5 mm K-type coated thermocouples at depth ranges from 1 to 4 mm below the coated surface. The experimental set-up is schematically shown in Fig. 2, details can be found in Ref 3.

Temperatures measured at various depths under the surface of the sample are shown in Fig. 3 and 4. In the case of Fig. 3 they represent the overall thermal effect of coating deposition. This thermal effect consists of all three above-mentioned processes participating in sample heating (hot gas flow, thermal and kinetic energy of powder). In further text and figures this will be briefly denoted as spraying. In the case of Fig. 4, the temperatures manifest the effect of hot gas flow without deposition of a coating. This means only the first assigned heating process (hot gas flow) takes part in the sample heating. In further text and figures it will be briefly denoted as preheating, because such process is technologically used to preheat the samples to a selected temperature prior to coating deposition.

Concerning the spraying, the initial temperature of the sample measured by all thermocouples was 321 K. In the case of preheating, the initial temperature was 316 K. During approximately 0.5 s maximum temperatures were reached and then the temperature slowly decreased. Differences in the temperature evolutions are caused by the different depths of sensors under the surface and their spatial distribution along the HVOF gun axis trajectory. These temperatures are the input values for the surface temperature evaluation by the Exodus method.

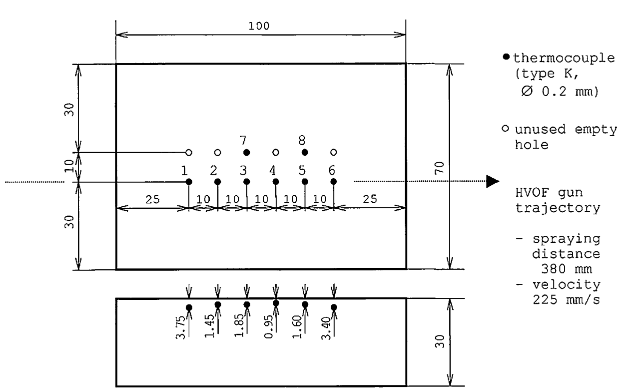

Fig. 2 The shape of the sample with locations of embedded thermocouples for the temperature measurement used in solving the inverse problem

3.2 Simulation Model Description

Measured six temperature evolutions (thermocouples nos. 1 to 6 in Fig. 2) were used to solve the inverse problem in order to evaluate surface temperatures.

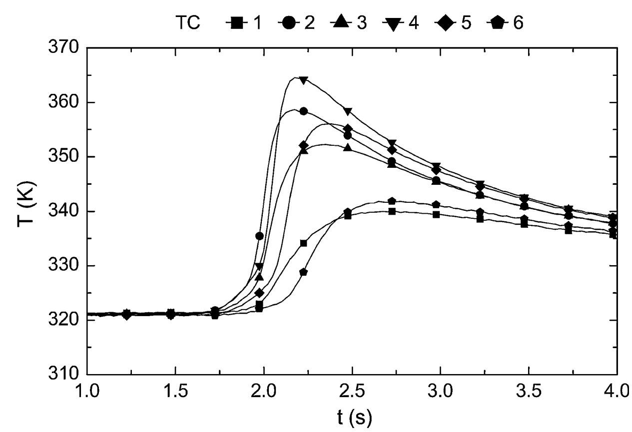

Fig. 3 Temperatures measured by thermocouples nos. 1 to 6 (TC x) at various depths under the sample surface during spraying

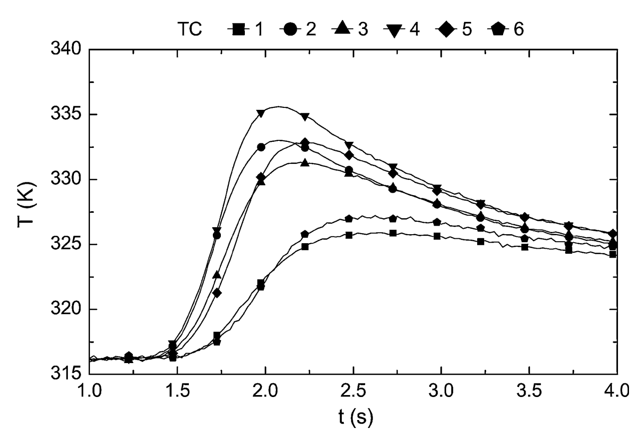

Fig. 4 Temperatures measured by thermocouples nos. 1 to 6 (TC x) at various depths under the sample surface during preheating

A simple model constructed is based on assumption of one-dimensional heat conduction. The computational grid is composed of 33 nodes (3×11), rectangular and with non-uniform spacing along the depth from the surface. One measured temperature evolution is considered in the center node of the first subsurface layer. Therefore different computational grid is used for evaluations with different depths of thermocouples. The computation has been performed using Eq 28.

Thermal properties of the sample are assumed $\lambda = 43$ W m^{-1} K^{-1}, $c = 500$ J kg^{-1} K^{-1}, $\rho = 7800$ kg m^{-3}. The time step for the simulation was $\Delta\tau = 0.025$ s, in non-dimensional form $\Delta Fo = 2.76 \times 10^{-7}$.

3.3 Surface Temperature Evaluation

Results of the sample surface temperature evaluation by the Exodus method are shown in Fig. 5 and 6. Temperatures measured by thermocouples are used as input values in solving the inverse problem. Surface temperature evolution over time is the result of the computational procedure.

Temperatures in Fig. 5 show the results for spraying, temperatures in Fig. 6 show the results for preheating. The comparison of all curves in one figure reveals the magnitude of the surface temperature is not dependent on the depth where the input temperature is measured. Higher oscillations appear in the case of surface temperatures corresponding to higher depth of the input measured temperature. The oscillations are usually the main limitation of the Exodus inverse method giving the maximum depth, where the input measured temperature evolution is considered. The phenomenon is caused by the amplification of initial perturbations in the transient inverse problems as the method tries to correct deviation originated in the previous step. It is not the case of stationary inverse problems.

The results show that the surface temperature increased by about 80 K during one pass of the gun over the sample in the case of spraying and about 25 K in the case of preheating. The rate of the temperature increase is proportional to the heat flux to the sample surface. The maximum heat flux is reached at the time of the maximum heating rate and just as the gun axis travels over the measured location. Maximum surface temperature is reached at some distance behind the gun axis.

3.4 Verification of Results

In order to verify the results of the inverse problem, two types of comparisons were considered.

The first one is a comparison of the temperatures computed by the Exodus method (direct problem) with the original temperatures measured by thermocouples inside the sample. Surface temperatures evaluated as the inverse problem by the Exodus method are used as the input values to the solution of the direct problem. Results of the direct problem solved also by the Exodus method are temperatures at certain depths under the sample surface identical to the locations of thermocouples. If the method works correctly, the temperatures should agree with the measured ones. The comparison in the case of spraying is shown in Fig. 7, and in Fig. 8 for the preheating. This is only a simple verification that enables to show errors in the method computational procedures. Therefore, a comparison with another method should be done to verify the Exodus method accuracy.

Thus, the second verification is based on the comparison of surface temperature evolutions provided by the Exodus method and by the model using the FEM method (Ref 3). In both cases, it is a solution of the inverse problem with the same input measured temperatures. The comparison for spraying and for preheating is shown in Fig. 9 and reveals good agreement of the results provided by both methods.

3.5 Application of Results

Results of these simple computations of the inverse problem and the evaluation of surface temperature have been used in the experimental investigation of HVOF processes by an infrared camera system. Comparison of

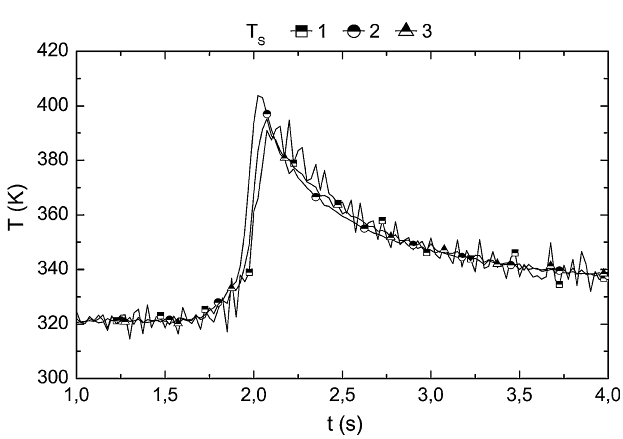

Fig. 5 Sample surface temperature during spraying evaluated by the Exodus method (inverse problem) based on the measured subsurface temperatures referred to thermocouple nos. 1 to 6

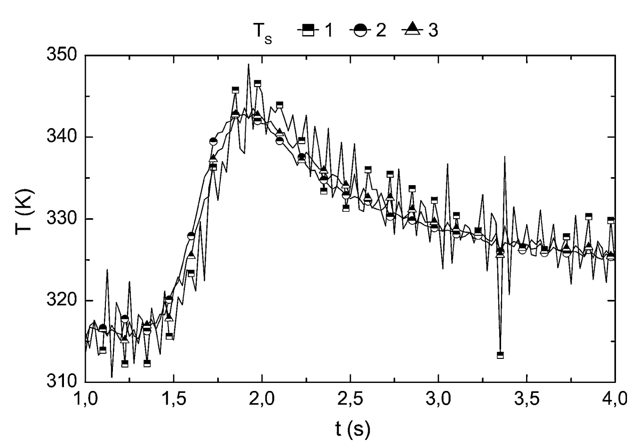

Fig. 6 Sample surface temperature during preheating evaluated by the Exodus method (inverse problem) based on the measured subsurface temperatures referred to TC nos. 1 to 3

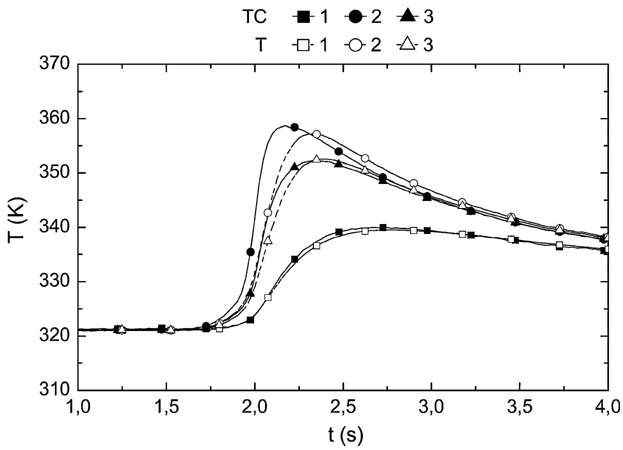

Fig. 7 Comparison of temperatures computed by the Exodus method (direct problem) (T) with temperatures measured by thermocouples nos. 1 to 3 (TC) at various depths under the sample surface during spraying

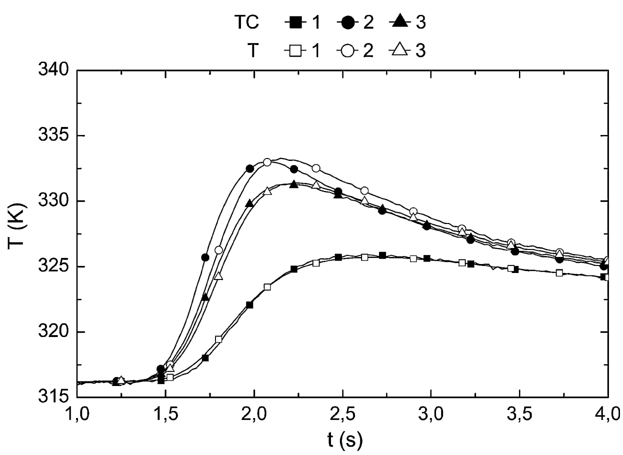

Fig. 8 Comparison of temperatures computed by the Exodus method (direct problem) (T) with temperatures measured by thermocouples nos. 1 to 3 (TC) at various depths under the sample surface during preheating

the computed temperatures with temperatures non-contactly measured in the coating deposition area has allowed determining measurement errors caused by radiation of hot gas and particle stream from the HVOF gun interfering with radiation of the surface. The measured surface temperature during deposition of the first layer on the substrate has been identified about 70 K higher than the surface temperature provided by the inverse problem computation.

In general, such inverse problem computations can be used to identify unknown boundary conditions of all types.

The unknown heat flux on the surface can additionally be determined to the unknown surface temperature. Therefore, the heat flux is computed based on temperature difference determined on the surface and in some depth δ, for example 10^{-5} m, below the surface. First,

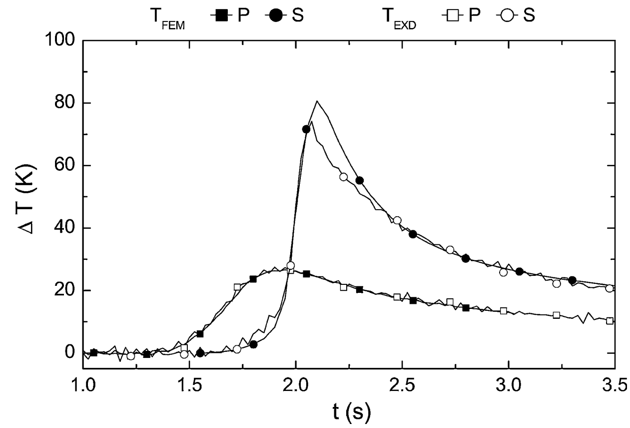

Fig. 9 Comparison of increase in sample surface temperatures evaluated by the Exodus method (inverse problem) (EXD) and by the FEM method (inverse problem) (FEM) (Ref 3) for spraying (S) and preheating (P)

surface temperature (T_1) is calculated as the inverse problem on normal grid. Second, surface temperature (T_2) is calculated on grid, where the surface nodes are shifted by δ. Finally, the heat flux is computed by the equation

$$q = (T_1(t) - T_2(t)) \cdot \lambda \cdot \delta^{-1}. \quad \text{(Eq 29)}$$

Considering the other types of boundary conditions (convection, radiation), these can be evaluated based on the already computed surface temperature and heat flux. If, for example, ambient temperature evolution is known (measured), the boundary condition parameters such as radiation emissivity or convection heat transfer coefficient can be determined.

4. Conclusions

The Exodus method provides a straightforward means of solving indirect problems. Although the method is probabilistic in its approach, it is not subject to randomness as other Monte Carlo techniques, because it does not involve the use of a pseudo-random generation subroutine. Considering thermal spraying technology, the method is able, in conjunction with temperature measurement inside samples, to determine surface temperatures and heat fluxes during deposition. It was also found that the Exodus method gives a solution as accurate as that obtained with the finite element method. If necessary, the method can also be modified to consider multi-layer material structures.

Acknowledgment

This paper is based upon work sponsored by the Ministry of Education, Youth and Sports of the Czech Republic under research project no. MSM4977751302.

Peer Reviewed

References

1. P. Fauchais, Understanding Plasma Spraying, *J. Phys. D: Appl. Phys.*, 2004, **37**, p R86-R108
2. D. Cheng, G. Trapaga, J.W. McKelliget, and E.J. Lavernia, Mathematical Modelling of High Velocity Oxygen Fuel Thermal Spraying of Nanocrystalline Materials: An Overview, *Modelling Simul. Mater. Sci. Eng.*, 2003, **11**, p R1-R31
3. M. Honner, P. Cerveny, V. Franta, and F. Cejka, Heat Transfer During HVOF Deposition, *Surf. Coat. Technol.*, 1998, **106**, p 94-99
4. O.M. Alifanov, E.A. Artyukhin, and S.V. Rumyantsev, *Extreme Methods for Solving Ill-Posed Problems with Applications to Inverse Heat Transfer Problems*, Begell House, New York, 1995
5. J.J. Gonzalez, P. Freton, M. Masquere, X. Franceries, and F. Lago, Plasma Heat Transfer: Inverse Methods for Optimizing the Measurements, *J. High Temp. Mater. Processes*, 2005, **9**(4), p 599-605
6. R.W. Lewis, P. Nithiarasu, and K. Seetharamu, *Fundamentals of the Finite Element Method for Heat and Fluid Flow*, Wiley, New York, 2004
7. J. Mackerle, Coatings and Surface Modification Technologies: A Finite Element Bibliography (1995–2005), *Modelling Simul. Mater. Sci. Eng.*, 2005, **13**, p 935-979
8. J. Sladek, V. Sladek, and Y.C. Hon, Inverse Heat Conduction Problems by Meshless Local Petrov–Galerkin Method, *Eng. Anal. Bound. Elem.*, 2006, **30**, p 650-661
9. A. Haji-Sheikh, The Monte Carlo Method, *Handbook of Numerical Heat Transfer*, W.J. Minkowytz, E.M. Sparrow, G.E. Schneider, and R.H. Pletcher, Ed., Wiley, New York, 1988, p 673-722
10. A.F. Emery and W.W. Carson, A Modification to the Monte Carlo Method—The Exodus Method, *J. Heat Transf.*, 1968, **90**, p 328-332
11. J.G. Kemeny and J.L. Snell, *Finite Markov Chains*, D. Van Nostrand Co., Inc., Princeton, NJ, 1960, p 69-94
12. M.N.O. Sadiku, S.O. Ajose, and Z. Fu, Applying the Exodus Method to Solve Poisson's Equation, *IEEE Trans. Microwave Theory Tech.*, 1994, **42**(4), p 661-666
13. M.N.O. Sadiku and D.T. Hunt, Solution of Dirichlet Problems by the Exodus Method, *IEEE Trans. Microwave Theory Tech.*, 1992, **40**(1), p 89-95